Probing the Heme Iron Coordination Structure of Pressure-Induced Cytochrome $P420_{cam}$†

Susan A. Martinis,‡ Steven R. Blanke,‡ Lowell P. Hager, and Stephen G. Sligar*

Department of Biochemistry, School of Chemical Sciences, University of Illinois, Urbana, Illinois 61801

Gaston Hui Bon Hoa

INSERM-INRA, U310, Institute de Biologie Physico-Chimique, 13 rue Pierre et Marie Curie, 75005 Paris, France

John J. Rux§ and John H. Dawson*

Department of Chemistry and Biochemistry and School of Medicine, University of South Carolina, Columbia, South Carolina 29208

Received June 24, 1996; Revised Manuscript Received September 4, 1996⊗

ABSTRACT: Cytochrome $P450_{cam}$ was subjected to high pressures of 2.2 kbar, converting the enzyme to its inactive form, $P420_{cam}$. The resultant protein was characterized by electron paramagnetic resonance, magnetic circular dichroism, circular dichroism, and electronic absorption spectroscopy. A range of exogenous ligands has been employed to probe the coordination structure of $P420_{cam}$. The results suggest that conversion to $P420_{cam}$ involves a conformational change which restricts the substrate binding site and/or alters the ligand access channel. The reduction potential of $P420_{cam}$ is essentially the same in the presence or absence of camphor (-211 ± 10 and -210 ± 15 mV, respectively). Thus, the well-documented thermodynamic regulation of enzymatic activity for $P450_{cam}$ in which the reduction potential is coupled to camphor binding is not found with $P420_{cam}$. Further, cyanide binds more tightly to $P420_{cam}$ ($K_d = 1.1 \pm 0.1$ mM) than to $P450_{cam}$ ($K_d = 4.6 \pm 0.2$ mM), reflecting a weakened iron−sulfur ligation. Spectral evidence reported herein for $P420_{cam}$ as well as results from a parallel investigation of the spectroscopically related inactive form of chloroperoxidase lead to the conclusion that a sulfur-derived proximal ligand is coordinated to the heme of ferric cytochrome $P420_{cam}$.

The chemical mechanism which enables the family of cytochromes P450 to catalyze unique oxidative reactions has been extensively probed by a combination of physical, chemical, and genetic methodologies (Dawson & Sono, 1987; Martinis et al., 1990; Ortiz de Montellano, 1995; Mueller et al., 1995). The monooxygenase activity of P450 has been primarily attributed to the presence of an unusual proximal heme ligand, a thiolate sulfur donor provided by a cysteinate residue (Poulos et al., 1985; Dawson, 1988). This distinct ligand has been found in only a few other enzymes, including chloroperoxidase from *Caldariomyces fumago* (Dawson & Sono, 1987; Blanke & Hager, 1988; Sundaramoorthy et al., 1995) and NO synthase (White & Marletta, 1992).

The cytochrome P450 Fe−S bond yields distinct physical characteristics that have been evaluated by a number of spectroscopic methods (Dawson & Sono, 1987). Theoretical calculations have suggested a molecular basis for these unusual spectral transitions (Hanson et al., 1976; Jung, 1985). Although chemical mechanisms for the monooxygenase reaction have been proposed on the basis of the investigations cited above and by analogy to peroxidases and heme model systems (Dawson, 1988; Martinis et al., 1989; Ortiz de Montellano, 1995), the precise catalytic role of the proximal thiolate remains ill-defined due to the highly transient nature of the P450 intermediate(s) that follows oxy-P450.

The cytochromes P450 undergo a universal transition to a stable but inactive species known as cytochrome P420. Ferrous−CO P420 has its Soret absorption peak at 420 nm rather than at 450 nm as is characteristic of P450. Numerous chemical and physical techniques, including increased temperatures or pressures, or the addition of salts, denaturants, or organic solvents (Imai & Sato, 1967; Yu & Gunsalus, 1974; Fisher et al., 1985; Hui Bon Hoa et al., 1989) convert P450 to P420. P420 can sometimes be converted back to P450 by incubation with thiols, spermine, dimethyl sulfoxide, polyols, and/or native substrates (Ichikawa & Yamano, 1967; Yu & Gunsalus, 1974; Hui Bon Hoa et al., 1989, 1990). A few of the cytochromes P420 have been examined by electronic absorption (Yu & Gunsalus, 1974; Hui Bon Hoa et al., 1989), resonance Raman (Champion et al., 1978; Ozaki et al., 1978; Wells et al., 1992), magnetic circular dichroism (MCD)[1] (Collman et al., 1976), circular dichroism (Hong et

† This work was supported by National Institutes of Health Grants GM31756 and GM33775 (to S.G.S.), GM7768 (to L.P.H.), and GM26730 (to J.H.D.) and by INSERM-INRA (U310) and the French Ministry of Research under Grant 85.T.0717 (to G.H.B.H.). The Illinois EPR Research Center was funded by National Institutes of Health Grant RR-01811. The JASCO J-500 spectrometer was purchased under National Institutes of Health Grant RR-03960 (to J.H.D.), and the electromagnet was obtained with a grant from Research Corporation (to J.H.D.).

* To whom correspondence should be addressed.

‡ Present address: Department of Biochemical and Biophysical Sciences, University of Houston, Houston, TX 77204-5934.

§ Present address: Wistar Institute, Philadelphia, PA 19104.

⊗ Abstract published in *Advance ACS Abstracts,* October 15, 1996.

[1] Abbreviations: MCD, magnetic circular dichroism; EPR, electron paramagnetic resonance.

S0006-2960(96)01511-5 CCC: $12.00

al., 1983), laser photolysis (Tian et al., 1995), and EPR (Ebel et al., 1975; Lipscomb, 1980) for comparison to the native protein.

The structural alterations that occur during inactivation of P450 may pinpoint the features that are important for catalytic activity and provide insight into the nature of the putative intermediates. Speculation concerning the structure of P420 revolves around the proximal heme iron ligand. In particular, it has been suggested that a conformational change substitutes histidine for the proximal cysteine, yielding a myoglobin-like heme coordination structure. Alternatively, theoretical calculations have indicated that the proximal thiolate may be protonated, resulting in a weak thiol ligand (Hanson et al., 1976), or that the Fe−S bond might be weakened by lengthening (Jung et al., 1979; Jung, 1985). In reality, there is little experimental evidence in the literature to distinguish these hypotheses.

To address this issue, we have undertaken an extensive spectroscopic investigation to characterize cytochrome $P420_{cam}$ more thoroughly. As previously reported, $P420_{cam}$ can be generated using high pressure (Marden & Hui Bon Hoa, 1982, 1987; Fisher et al., 1985; Hui Bon Hoa et al., 1989). The resultant protein is stable and has been examined herein by electronic absorption, MCD, and EPR spectroscopy. Pressure-induced $P420_{cam}$ has been previously analyzed using resonance Raman spectroscopy (Wells et al., 1992). Like resonance Raman, MCD and EPR spectroscopy are frequently used to probe the coordination structure of heme iron proteins because the methods are very sensitive to changes in the spin and ligation state of the heme iron (Dawson & Dooley, 1989; Sono et al., 1991). Exogenous ligands and substrate analogs have been utilized in the present study to probe the coordination structure of the $P420_{cam}$ heme iron. As camphor has a significant effect on the reduction potential of $P450_{cam}$ (Sligar, 1976; Sligar & Gunsalus, 1976), we have examined the reduction potential of $P420_{cam}$ in the presence and absence of camphor. In summary, we report herein alterations in the heme environment and coordination structure that directly affect the ability of $P450_{cam}$ to bind and turn over camphor.

EXPERIMENTAL PROCEDURES

Unless otherwise specified, standard chemical reagents were purchased from commercial sources. Isobornyl mercaptan was synthesized as previously described (Murray & Dus, 1980). Cytochrome $P450_{cam}$ was fermented and isolated from either its original native source, *Pseudomonas putida* (Gunsalus & Wagner, 1978), or the *Escherichia coli*-expressed clone (Unger et al., 1986). The protein was purified to an R_z value of greater than 1.40 as determined by absorption spectroscopy. P420 formation was accomplished by pressure treatment of camphor-free $P450_{cam}$ as previously described (Hui Bon Hoa et al., 1989; Martinis, 1990)

Electronic absorption spectra were obtained using a Hewlett-Packard 8450A or a Varian/Cary 210 or 219 spectrophotometer. The Varian/Cary 210 spectrophotometer was equipped with a Lauda circulator and computer interfaced to an IBM PC.

EPR spectra were recorded in the University of Illinois EPR Research Center. Spectra were collected on a Bruker ER 220D-SRC instrument equipped with a Bruker microwave bridge ER042MRH, helium dewar, Varian gaussmeter, and EIP microwave 548A frequency meter. Experimental conditions included a 100 kHz modulation frequency, 16 dB of microwave power, and a 500 s total scan time. Data manipulations were carried out with an IBM PC and in-house software (Morse, 1987).

The MCD and circular dichroism spectra were recorded on a JASCO J-500A spectropolarimeter equipped with a JASCO MCD-1B electromagnet operated at 1.41 T. The J-500A instrument was interfaced to an IBM PS/2 model 50 PC by a JASCO IF-500-2 interface unit. Electronic absorption spectra recorded before and after MCD/CD analysis showed less than 5% change. Data acquisition and handling were performed as previously described (Huff et al., 1993). The MCD spectra reported are the average of two to four scans and have been corrected for natural circular dichroism.

Reduction potentials were measured spectrophotometrically (Dutton, 1978) by a modification of the previously described method (Sligar & Gunsalus, 1976). Specifically, a solution containing 50 mM potassium phosphate (pH 7.0), 10 mM ethylenediaminetetraacetic acid, 10 μM brilliant alizarin blue, and 10 μM $P420_{cam}$ was degassed by a vacuum pump in a Thunberg cuvette. The solution was made 20 μM in camphor when determining substrate effects on the $P420_{cam}$. Reduction was induced by periodic 15−60 s exposure to light. The redox equilibrium between the dye and protein was monitored at 602 and 391 nm, respectively, on the Hewlett-Packard spectrophotometer. Complete reduction was ensured by the addition of sodium dithionite crystals.

Native electron transfer reactions of the camphor hydroxylase system which were used to determine product formation and NADH consumption rates were carried out exactly as described previously (Martinis, 1990; Martinis et al., 1989).

The K_d of cyanide binding for substrate-free $P450_{cam}$ was measured using difference spectroscopy by the procedure outlined for camphor binding (Martinis et al., 1989; Martinis, 1990). Specifically, the maximum at 438 nm and the minimum at 427 nm were measured after 0.5−1.0 μL additions of 10 mM cyanide. The binding of cyanide to $P420_{cam}$ was followed by monitoring the increase in intensity at 422 nm in the absolute absorption spectrum. The absorbance at 700 nm was employed to adjust the data for background. The data were interpreted graphically as described by Weber (1973).

The NO complex of ferric $P420_{cam}$ or $P450_{cam}$ was produced by the passage of NO gas through a saturated solution of KOH followed by gentle bubbling into the degassed protein solution (Ebel et al., 1975). The ferrous−NO complexes were generated by the addition of 10 mL of degassed 10 mM dithionite solution.

RESULTS

Cytochrome $P450_{cam}$ is efficiently converted to P420 under pressures of 2.0−2.4 kbar. The electronic absorption spectrum of ferric $P420_{cam}$ displays a prominent δ band at 367 nm, a Soret band at 422 nm, an α band (566 nm) which is a shoulder to the more intense β band (541 nm), and an additional weak absorption band at 651 nm (Figure 1, top). The relative intensities of the 422 and 376 nm maxima varied for different P420 preparations. When the native substrate camphor is added to ferric $P450_{cam}$, the Soret band at 417

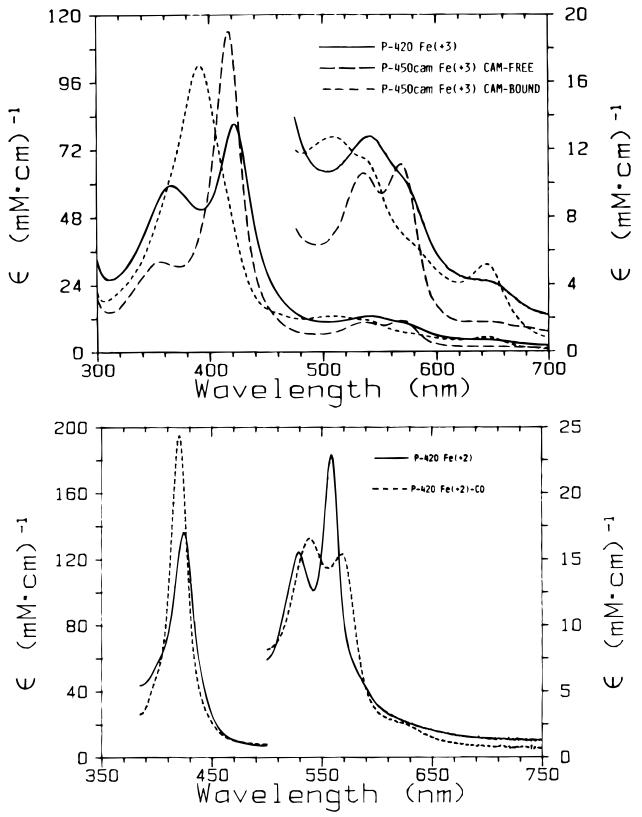

FIGURE 1: Electronic absorption spectra at 4 °C. (top) (—) Pressure-induced ferric $P420_{cam}$ (8.7 μM) in 50 mM Tris (pH 7.4), (— —) camphor-free ferric $P450_{cam}$ (13.5 μM) in 100 mM KP_i (pH 7.0), and (---) camphor-bound ferric $P450_{cam}$ (19.6 μM) in 100 mM KP_i (pH 7.0) and 60 μM camphor. (bottom) Pressure-induced (—) ferrous and (— —) ferrous—CO $P420_{cam}$ (8.7 μM) in 50 mM Tris (pH 7.4).

nm shifts to 391 nm, reflecting a displacement of water from the active site (Poulos et al., 1986). However, as with acetone-generated $P420_{cam}$ (Yu & Gunsalus, 1974), camphor addition to pressure-induced cytochrome $P420_{cam}$ does not perturb the absorption spectrum.

Dithionite reduction of ferric $P420_{cam}$ yields the ferrous protein which has a Soret absorption transition at 424 nm along with bands at 530 and 558 nm in the visible region (500—700 nm). Addition of CO leads to the characteristic absorption peak at 420 nm of the ferrous—CO state as well as maxima at 540 and 572 nm (Figure 1, bottom). Additionally, a distinct trough at 435 nm is observed in the ferrous—CO minus ferrous difference absorption spectrum. In contrast, the difference spectrum of $P450_{cam}$ displays a single visible band at 550 nm as well as the unique maximum at 446 nm (Gunsalus & Wagner, 1978).

The inactivation of $P450_{cam}$ by pressure is accompanied by a complete loss of camphor turnover and NADH consumption in the presence of the native redox partners, putidaredoxin and putidaredoxin reductase. Small amounts ($\leq$5%) of native $P450_{cam}$ contamination are difficult to detect by absolute absorption spectroscopy but can be seen in the ferrous—CO minus ferrous difference spectrum as slight deviations in the minimum or shoulders arising on the positive slope of the trough.

The EPR spectra of pressure-induced ferric $P420_{cam}$ in either the presence or absence of saturating camphor concentrations are essentially identical to those of substrate-free ferric $P450_{cam}$ (Lipscomb, 1980). The *g* values observed

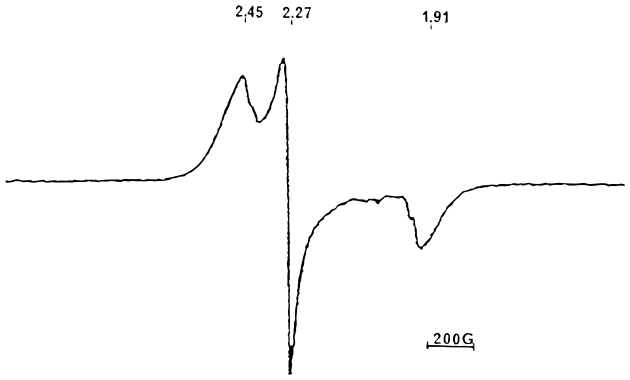

FIGURE 2: EPR spectrum at 35.8 K of pressure-induced ferric $P420_{cam}$ in 50 mM Tris, (pH 7.4). Conditions: time constant, 0.02 s; modulation amplitude, 12.5 G; microwave power, 16 dB; and microwave frequency, 9.492 GHz. The small signals around $g = 2$ are due to cavity contamination.

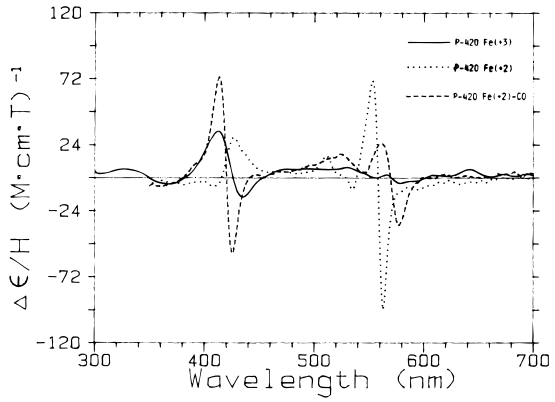

FIGURE 3: MCD spectra in 50 mM Tris at 4 °C and pH 7.4. (—) Pressure-induced ferric $P420_{cam}$ (8.7 μM), (— —) pressure-induced ferrous $P420_{cam}$ (8.7 μM), and (— — —) pressure-induced ferrous—CO $P420_{cam}$ (8.7 μM).

at 2.45, 2.27, and 1.91 (Figure 2) match those of acetone-generated $P420_{cam}$ (2.42, 2.25, and 1.91; Lipscomb, 1980) and are essentially unchanged upon increasing the pH to 9.0.

The MCD spectrum of ferric $P420_{cam}$ (Figure 3) exhibits a positive derivative-shaped feature in the Soret region (300—500 nm). However, it is not symmetrical, and the crossover point at 426 nm is red-shifted by 4 nm compared to the absorption maximum, likely reflecting the presence of more than one species. The visible region contains peaks at 529 and 566 nm. The spectrum is unaffected by the addition of camphor. The MCD spectrum of ferrous $P420_{cam}$ (Figure 3) is dominated by the visible region which displays an intense, positive derivative-shaped band with a crossover at 558 nm. A peak at 426 nm is centered on the Soret absorption maximum. Ferrous—CO $P420_{cam}$ has a MCD spectrum with a large positive derivative-shaped band centered at 420 nm, a peak at 523 nm, followed by another positive derivative-shaped band (Figure 3).

Various other substrates and exogenous ligands which bind to ferric $P450_{cam}$ were combined with $P420_{cam}$ to probe the heme iron coordination properties. Isobornyl mercaptan, a thiol analog of camphor, binds tightly to the heme iron of ferric $P450_{cam}$ ($K_d = 0.47$ μM; Murray & Dus, 1980) to give split Soret peaks that are characteristic of a bis-thiolate ligated ferric heme (Dawson & Sono, 1987). Second-derivative absorption spectroscopy indicates that, upon isobornyl mercaptan binding, water is completely displaced from the active site of $P450_{cam}$, thus mimicking camphor binding (Atkins &

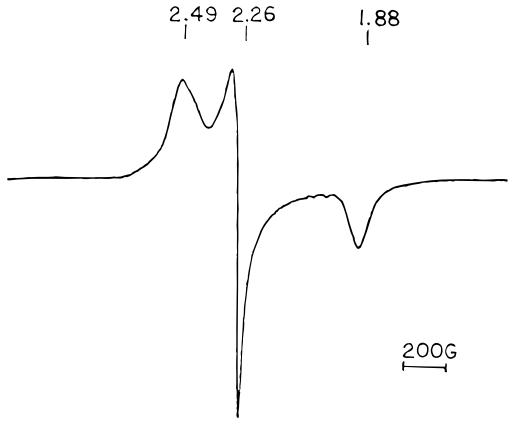

FIGURE 4: EPR spectrum at 13.9 K of imidazole-bound pressure-induced ferric $P420_{cam}$ in 50 mM Tris (pH 7.2) and 1 mM imidazole. Conditions: time constant, 0.16 s; modulation amplitude, 10 G; microwave power, 16 dB; and microwave frequency, 9.428 GHz. Note that the small signals around $g = 2$ reflect cavity contamination.

Sligar, 1990). Addition of isobornyl mercaptan to ferric $P420_{cam}$, however, fails to produce any absorption or EPR spectral changes, indicating that it cannot ligate at the iron center.

The electronic absorption, MCD, and EPR spectra of numerous $P450_{cam}$−ligand complexes have been documented (Dawson et al., 1982; Sono & Dawson, 1982; Dawson & Sono, 1987). Similarly, exogenous ligands were selected to probe the heme environment of pressure-induced $P420_{cam}$. Propanethiol, *p*-chlorothiophenol, and 2-mercaptoethanol each ligate to ferric $P450_{cam}$ via their thiol group (Dawson et al., 1982) to yield bis-thiolate ferric heme adducts. Although excess quantities of the above thiols have been incubated with ferric $P420_{cam}$ at neutral and alkaline pH, no spectral evidence of binding was observed. The binding of nitrogenous donor ligands was also investigated. Azide, which binds to ferric $P450_{cam}$ with a K_d of 200 mM (Sono & Dawson, 1982), fails to perturb the absorption spectrum of ferric $P420_{cam}$. The absorption spectra of ferric and ferrous $P420_{cam}$ in buffer containing 0.14 M imidazole display bands at 418 and 538 nm and at 420, 530, and 558 nm, respectively. The EPR spectrum of ferric $P420_{cam}$ in the presence of imidazole (Figure 4) exhibits *g* values of 2.49, 2.26, and 1.88 that occur over a somewhat broader range than in the absence of imidazole (Figure 2). These may be compared to the *g* values of ferric−imidazole $P450_{cam}$ of 2.56, 2.27, and 1.87 (Dawson et al., 1982). The MCD spectrum of ferric $P420_{cam}$ shifts to a slightly higher energy in the Soret region in the presence of imidazole with little effect on the bands of the visible region. The MCD spectrum of the ferrous protein in imidazole-containing buffer is essentially identical to that of ferrous ligand-free $P420_{cam}$. The ferric−NO $P420_{cam}$ adduct is very unstable. Ferrous−NO $P420_{cam}$ yields a split EPR spectrum (Figure 5) identical to that of ferrous−NO $P420_{cam}$ generated by acetone treatment (Ebel et al., 1975), which has *g* values of 2.00, 2.01, and 2.02.

Cyanide concentrations of greater than 10 mM shift the Soret absorption band of ferric $P420_{cam}$ from 420 to 422 nm, concurrent with an increase in the extinction coefficient; the band in the visible region occurs at 552 nm. When the protein is reduced in the presence of cyanide, the Soret transition is further red-shifted to 430 nm, again with an increase in intensity. The α and β bands appear at 534 and

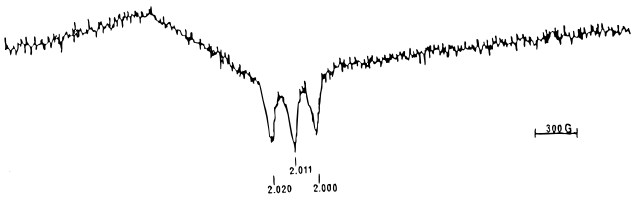

FIGURE 5: EPR spectrum at 77 K of pressure-induced ferrous−NO $P420_{cam}$. See the Experimental Procedures for the method of complex formation. Conditions: time constant, 0.08 s; modulation amplitude, 16 G; microwave power, 16 dB; and microwave frequency, 9.294 GHz.

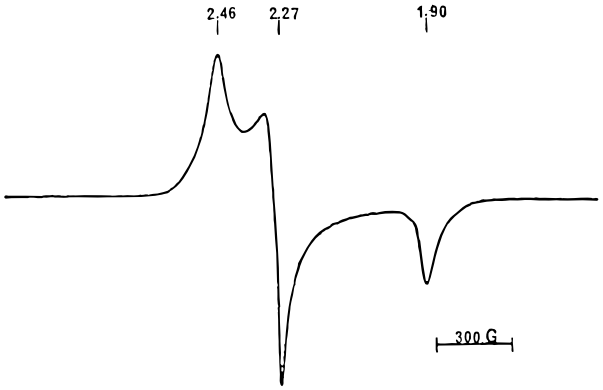

FIGURE 6: EPR spectrum at 13.9 K of metyrapone-bound pressure-induced ferric $P420_{cam}$ in 50 mM KP_i (pH 7.0) and 500 μM metyrapone. Conditions: time constant, 0.04 s; modulation amplitude, 10 G; microwave power, 16 dB; and microwave frequency, 9.432 GHz.

562 nm, respectively. When the ferrous protein is bubbled with CO, cyanide is displaced. The EPR spectrum of ferric $P420_{cam}$ in the presence of cyanide has *g* values of 2.61, 2.48, 2.28, and 1.89 that are suggestive of the presence of more than one species. This is most likely due to incomplete binding of the ligand. For comparison, the cyanoferric $P450_{cam}$ has *g* values of 2.59, 2.30, and 1.81 (Tsai *et al.*, 1970). The MCD spectra of ferric and ferrous $P420_{cam}$ are also perturbed in the presence of cyanide. The spectrum of the ferric protein has a more intense derivative-shaped Soret transition that is shifted to lower energy. The K_d value for the ferric $P420_{cam}$−cyanide complex is 1.1 ± 0.1 mM, about 4 times smaller than that measured under similar conditions for cyanide binding to ferric $P450_{cam}$ (4.6 ± 0.2 mM) (Sono & Dawson, 1982).

The pyridine derivative metyrapone is a common P450 inhibitor (Poulos & Howard, 1987). Although the absorption spectrum and the EPR *g* values of the ferric $P420_{cam}$−metyrapone complex resemble those for ferric $P420_{cam}$ in the absence of metyrapone, the shape of the EPR spectrum is distinct (Figure 6). Upon reduction, the Soret band in the absorption spectrum increases in intensity and is blue-shifted 4 nm to 416 nm. The α and β bands are found at 524 and 556 nm, respectively. In contrast to the ferrous−cyanide complex, CO does not displace metyrapone. The primary effect on the MCD spectrum of ferric $P420_{cam}$ following addition of metyrapone is an increase in the intensity and a slight shift to higher energy for the derivative-shaped Soret transition, with little or no effect on the trough that corresponds to the δ band at 367 nm or the features in the visible region. When the protein is reduced in the presence of metyrapone, the MCD transitions are shifted to slightly higher energy relative to those present in the spectrum of ferrous $P420_{cam}$.

The reduction potentials for $P450_{cam}$ determined by spectrophotometric titration (Dutton, 1978) have been previously reported to be approximately −300 mV for the substrate-free form and −170 mV for the camphor-bound protein (Sligar & Gunsalus, 1976). These values were redetermined to be −330 and −163 mV using the same dyes, safranine T and brilliant alizarin blue, respectively. The reduction potential for $P420_{cam}$, determined using brilliant alizarin blue, shifts to -211 ± 10 mV and is unaffected by addition of camphor.

DISCUSSION

The cytochromes P450 all have a common inactive species known as P420. The defining property of P450 is the distinct "hyper" absorption spectrum of its ferrous−CO state with bands at 446 and 363 nm (Hanson et al., 1976), while ferrous−CO P420 has a single peak at 420 nm. An explanation for the hyper spectrum of ferrous−CO P450 in which a thiolate sulfur to π^* charge transfer transition mixes with the porphyrin $\pi-\pi^*$ transition has been proposed by Hanson et al. (1976). Protonation of the thiolate to give a thiol or displacement by another ligand, such as histidine, would eliminate the hyper absorption spectrum and give a peak at 420 nm as found in P420. In fact, both thiol- and imidazole-ligated ferrous−CO model complexes have Soret absorption peaks at 420 nm (Collman et al., 1976). A third possible explanation for the 420 nm absorption peak in ferrous−CO P420 comes from work by Jung (Jung et al., 1979; Jung, 1985), who concludes that the hyper absorption spectrum in ferrous−CO P450 depends strongly on the Fe−S(thiolate) bond distance. Lengthening of that bond by 0.2 Å could induce the spectral transition of ferrous−CO P450 to P420.

In the present study, $P420_{cam}$ has been produced through exposure to high pressures. This method efficiently and quickly produces large amounts of $P420_{cam}$ requiring no further purification. The resultant protein has been previously studied by resonance Raman spectroscopy (Wells et al., 1992) and is characterized herein by electronic absorption, MCD, and EPR spectroscopy and by electrochemistry to provide insight into the alterations to $P450_{cam}$ upon inactivation. The methods used in this study, as in the previous resonance Raman report (Wells et al., 1992), reveal no spectral perturbations or redox changes for ferric $P420_{cam}$ upon the addition of camphor. Thus, $P420_{cam}$ cannot bind camphor and lacks the camphor-dependent regulation of the redox equilibria of $P450_{cam}$ (Sligar, 1976).

Absorption, MCD, EPR, and resonance Raman spectroscopy reveal that ferric $P420_{cam}$ contains a mixture of ligation states. Specifically, resonance Raman spectroscopy indicates that the ferric state contains high-spin, five-coordinate and low-spin, six-coordinate species (Wells et al., 1992) The low-spin species has been attributed to a heme iron ligated by the proximal thiolate and a water molecule. This conclusion is supported by the EPR spectrum (Figure 2) which is virtually identical to that of camphor-free $P450_{cam}$. Low-spin camphor-free ferric $P450_{cam}$ has been shown to contain either water or hydroxide as the ligand *trans* to cysteinate by X-ray crystallography (Poulos et al., 1986). Thomman and co-workers have recently used electron spin echo envelope modulation spectroscopy to demonstrate that the sixth ligand is water (Goldfarb et al., 1996; Thomman et al., 1995). Presumably at the low temperature of the EPR measurement (35.8 K), the high-spin component has converted to low-spin as occurs with chloroperoxidase (Dawson & Sono, 1987). The MCD spectrum of ferric $P420_{cam}$ (Figure 3) is also consistent with a mixture of two species. For the most part, the spectrum resembles those of nitrogen and oxygen donor ligand adducts of ferric $P450_{cam}$ (Dawson & Sono, 1987), i.e., low-spin six-coordinate thiolate-ligated complexes. The presence of a second species contributing to the absorption and MCD spectra of ferric $P420_{cam}$ is suggested by the unusually strong absorbance at 367 nm (Figure 1) similar to that observed in low-pH myoglobin which has a Soret maximum at 370 nm (Sage et al., 1991) and by the asymmetry in the Soret region of the MCD spectrum (Figure 3). The high-spin species cannot be five-coordinate thiolate-ligated since the Soret maximum for such a complex occurs at about 390 nm as found in high-spin ferric $P450_{cam}$.

Unlike $P450_{cam}$, $P420_{cam}$ has only a limited ability to bind ligands. Excellent $P450_{cam}$ ligands such as isobornyl mercaptan, *p*-chlorothiophenol, 2-mercaptoethanol, propanethiol, and azide do not bind to the $P420_{cam}$ heme iron. This suggests that the substrate/ligand binding site of $P420_{cam}$ is more restricted than that of $P450_{cam}$. Higher concentrations of planar compounds like metyrapone and imidazole or smaller ligands such as CO, NO, and cyanide appear to bind, producing spectra distinct from that of the protein prior to ligand addition. However, recent studies of geminant recombination of CO to ferrous $P420_{cam}$ indicate that the distal pocket environment is altered in the $P420_{cam}$ form (Tian et al., 1995). Sono and Dawson (1982) studied anion binding to ferric $P450_{cam}$ and found that the protein does not bind negatively charged ligands as well as myoglobin. The proximal thiolate ligand was proposed to contribute a greater amount of electron density to the iron than the proximal imidazole of myoglobin. Thus, anions bind much more weakly to $P450_{cam}$ than to myoglobin. Differences in the heme pocket polarity may also contibute to these differences. The K_d values for anion binding to $P420_{cam}$ are somewhat lower than those reported for native ferric $P450_{cam}$ (Sono & Dawson, 1982). Cyanide binds 4 times more tightly to ferric $P420_{cam}$ than to $P450_{cam}$, reflecting a weakening of the proximal thiolate ligation. However, the K_d of $P420_{cam}$ for cyanide (1.1 mM) does not approach that found for myoglobin (9.3 μM; Sono & Dawson, 1982), again arguing against replacement of the proximal thiolate with a histidine in the ferric state. Unlike ferric myoglobin, neither fluoride nor azide binds to the ferric $P420_{cam}$. The poor binding of small anions to ferric $P420_{cam}$ is consistent with a proximal ligand more negative than the histidine.

Chloroperoxidase also contains a proximal thiolate ligand (Dawson & Sono, 1987; Sundaramoorthy et al., 1995) and undergoes a P420-type transition (Lambeir & Dunford, 1983) to an inactive, C420, form whose ferrous−CO and −NO adducts spectroscopically resemble those of ferrous $P420_{cam}$ (Blanke et al., 1996). Like P450, chloroperoxidase can be reversibly converted to C420 under high pressures. Concurrent investigations of C420 have produced results similar to those found herein for $P420_{cam}$ suggesting that the proximal ligands of C420 and $P420_{cam}$ may be related (Blanke et al., 1996). In particular, ferric C420 appears to retain a thiolate proximal ligand but changes its ligand upon reduction. As $P450_{cam}$ and chloroperoxidase share little sequence homology,

it is unlikely that a parallel conformational change could replace the proximal cysteine with a histidine ligand upon reduction in both cases. While chloroperoxidase contains a histidine in the distal pocket (Blanke & Hager, 1990; Sundaramoorthy et al., 1995) as a potential ligand to the heme iron, there are no histidines near the heme iron of $P450_{cam}$ (Poulos et al., 1985). If the mechanisms of conversion for C420 and P420 are similar, it is more plausible to suggest that the proximal thiolate ligand is altered by protonation or by stretching the iron−sulfur bond upon reduction; these modifications could result from subtle conformational changes of the protein.

The coordination structure of $P420_{cam}$ changes significantly upon reduction. The MCD spectrum of ferrous $P420_{cam}$ is dominated by a sharp derivative-shaped curve in the visible region that resembles the feature seen in the spectra of ferrous cytochromes *c* and b_5 (Dawson & Dooley, 1989), low-spin, six-coordinate ferrous heme centers axially ligated by methionine and histidine or two histidines, respectively. Resonance Raman spectroscopy also supports the presence of a weaker ligand such as methionine, histidine, or water (Wells et al., 1992). Thus, it appears that the proximal thiolate ligand has been substituted by a more weakly electron-donating ligand. Resonance Raman spectroscopy also found a high-spin, five-coordinate population in equilibrium with the low-spin, six-coordinate species. The resonance Raman spectrum of the high-spin component was similar to that of low-pH deoxyferrous myoglobin which is axially liganded by a water molecule (Han et al., 1990). The MCD spectrum is also generally consistent with this observation. Non-thiolate-ligated high-spin ferrous heme centers, such as those found in deoxyferrous myoglobin, give rise to MCD spectra with minimal visible region intensity and an asymmetric derivative-shaped Soret region feature whose sign is the opposite of that of (positive at longer wavelength) the intense visible MCD band characteristic of low-spin ferrous complexes (Dawson & Dooley, 1989).

The addition of CO or NO further alters the coordination structure of ferrous $P420_{cam}$. The resonance Raman spectrum for ferrous−CO $P420_{cam}$ resembles that of low-pH ferrous−CO myoglobin (Wells et al., 1992). The MCD spectrum of ferrous−CO $P420_{cam}$ is consistent with either histidine or thiol *trans* to CO as both have the same MCD signature (Collman et al., 1976). Ferrous−NO $P420_{cam}$ yields a very distinct EPR spectrum (Figure 5) that has been attributed to a pentacoordinate heme which only contains an axial NO ligand (Wayland & Olson, 1974; Ebel et al., 1975; Trittelvitz et al., 1975; Desideri et al., 1984).

An intensive investigation of cytochrome $P420_{cam}$ has provided new information about its heme iron coordination structure, ligand binding properties, and redox properties. Ferric $P420_{cam}$ retains the thiolate ligand that is critical to P450 enzymatic activity but does not bind the normal substrate, camphor, or many typical heme iron ligands. Further, as the reduction potential of $P420_{cam}$ is unaffected by camphor, the control of spin state and reduction potential upon camphor binding to $P450_{cam}$ is lost in $P420_{cam}$. Upon reduction, the thiolate ligand is either protonated or lost. Taken together, these data indicate that the lack of enzymatic activity in $P420_{cam}$ is due to the combined inability to bind the substrate and to retain the proximal thiolate ligand in both ferric and ferrous oxidation states.

ACKNOWLEDGMENT

We thank Drs. Eric Coulter, Christiane Jung, Patrick S. Stayton, and Masanori Sono for insightful discussions, Jennifer Cheek for assistance in the preparation of the manuscript, and Dr. Ed Svastits for developing the computer-based MCD data-handling system. We also acknowledge Dr. William M. Atkins for providing the isobornyl mercaptan. In addition, we thank Dr. Gregorio Weber for furnishing the high-pressure equipment.

REFERENCES

Atkins, W. M., & Sligar, S. G. (1990) *Biochemistry 29,* 1271−1275.
Blanke, S. R., & Hager, L. P. (1988) *J. Biol. Chem. 263,* 18739−18743.
Blanke, S. R., & Hager, L. P. (1990) *J. Biol. Chem. 265,* 12455−12461.
Blanke, S. R., Martinis, S. M., Sligar, S. G., Hager, L. P., Rux, J. R., & Dawson, J. H. (1996) *Biochemistry 35,* 14537−14543.
Champion, P. M., Gunsalus, I. C., & Wagner, G. C. (1978) *J. Am. Chem. Soc. 100,* 3744−3751.
Collman, J. P., Sorrell, T. N., Dawson, J. H., Trudell, J. R., Bunnenberg, E., & Djerassi, C. (1976) *Proc. Natl. Acad. Sci. U.S.A. 73,* 6−10.
Dawson, J. H. (1988) *Science 240,* 433−439.
Dawson, J. H., & Sono, M. (1987) *Chem. Rev. 87,* 1257−1273.
Dawson, J. H., & Dooley, D. M. (1989) in *Iron Porphyrins, Part III* (Lever, A. B. P., & Gray, H. B., Eds.) pp 1−135, VCH Publishers, New York.
Dawson, J. H., Andersson, L. A., & Sono, M. (1982) *J. Biol. Chem. 257,* 3606−3617.
Desideri, A., Meier, U. T., Winterhalter, K. H., & Di Iorio, E. E. (1984) *FEBS Lett. 166,* 378−380.
Dutton, L. H. (1978) *Methods Enzymol. 54,* 411−435.
Ebel, R. E., O'Keeffe, D. H., & Peterson, J. A. (1975) *FEBS Lett. 55,* 198−201.
Fisher, M. T., Scarlata, S. F., & Sligar, S. G. (1985) *Arch. Biochem. Biophys. 240,* 456−463.
Goldfarb, D., Bernardo, M., Thomman, H., Kroneck, P. M. H., & Ullrich, V. (1996) *J. Am. Chem. Soc. 118,* 2686−2693.
Gunsalus, I. C., & Wagner, S. G. (1978) *Methods Enzymol. 52,* 166−188.
Han, N., Rousseau, D. L., Giacometti, G., & Brunori, M. (1990) *Proc. Natl. Acad. Sci. U.S.A. 87,* 205−209.
Hanson, L. K., Eaton, W. A., Sligar, S. G., Gunsalus, I. C., Gouterman, M., & Connell, C. R. (1976) *J. Am. Chem. Soc. 98,* 2672−2674.
Hong, Y.-S., Nonaka, Y., Kawata, S., Yamano, T., Miki, N., & Miyake, Y. (1983) *Biochim. Biophys. Acta 749,* 77−83.
Huff, A. M., Chang, C. K., Cooper, D. K., Smith, K. S., & Dawson, J. H. (1993) *Inorg. Chem. 32,* 1460−1466.
Hui Bon Hoa, G., Di Primo, C., Dondaire, I., Sligar, S. G., Gunsalus, I. C., & Douzou, P. (1989) *Biochemistry 28,* 651−656.
Hui Bon Hoa, G., Di Primo, C., Geze, M., Douzou, P., Kornblatt, J. A., & Sligar, S. G. (1990) *Biochemistry 29,* 6810−6815.
Ichikawa, Y., & Yamano, T. (1967) *Biochim. Biophys. Acta 131,* 490−497.
Imai, Y., & Sato, R. (1967) *Eur. J. Biochem. 1,* 419−426.
Jung, C. (1985) *Chem. Phys. Lett. 113,* 589−596.
Jung, C., Friedrich, J., & Ristau, O. (1979) *Acta Biol. Med. Germ. 38,* 363−377.
Lambeir, A. M., & Dunford, B. H. (1983) *Arch. Biochem. Biophys. 220,* 549−556.
Lipscomb, J. D. (1980) *Biochemistry 19,* 3590−3599.
Marden, M. C., & Hui Bon Hoa, G. (1982) *Eur. J. Biochem. 129,* 111−117.
Marden, M. C., & Hui Bon Hoa, G. (1987) *Arch. Biochem. Biophys. 253,* 100−107.
Martinis, S. A. (1990) Enzymatic Activation of Cytochrome $P\text{-}450_{cam}$, Ph.D. Thesis, University of Illinois, Urbana, IL.
Martinis, S. A., Atkins, W. M., Stayton, P. S., & Sligar, S. G. (1989) *J. Am. Chem. Soc. 111,* 9252−9253.

Martinis, S. A., Ropp, J. D., & Sligar, S. G. (1990) *Front. Biotransform. 4,* 54−86.

Morse, P. (1987) *Biophys. J. 51,* 440a.

Mueller, E. J., Loida, P. J., & Sligar, S. G. (1995) in *Cytochrome P450: Structure, Mechanism, and Biochemistry (Second Edition)* (Ortiz de Montellano, P. R., Ed.) pp 83−124, Plenum Press, New York.

Murray, R. I., & Dus, K. M. (1980) in *Microsomes, Drug Oxidations, and Chemical Carcinogenesis* (Coon, M. J., Conney, A. H., Estabrook, R. W., Gelboin, H. V., Gillette, J. R., & O'Brien, P. J., Eds.) pp 367−370, Academic Press, New York.

Ortiz de Montellano, P. R., Ed. (1995) *Cytochrome P450: Structure, Mechanism, and Biochemistry (Second Edition)*, Plenum Press, New York.

Ozaki, Y., Kitagawa, T., Kyogoku, Y., Imai, Y., Hashimoto-Yutsudo, C., & Sato, R. (1978) *Biochemistry 17,* 5826−5831.

Poulos, T. L., & Howard, A. J. (1987) *Biochemistry 26,* 8165−8174.

Poulos, T. L., Finzel, B. C., Gunsalus, I. C., Wagner, G. C., & Kraut, J. (1985) *J. Biol. Chem. 260,* 16122−16128.

Poulos, T. L., Finzel, B. C., & Howard, A. J. (1986) *Biochemistry 25,* 5314−5319.

Sage, J. T., Morikis, D., & Champion, P. M. (1991) *Biochemistry 30,* 1227−1236.

Sligar, S. G. (1976) *Biochemistry 15,* 5399−5406.

Sligar, S. G., & Gunsalus, I. C. (1976) *Proc. Natl. Acad. Sci. U.S.A. 73,* 1078−1082.

Sono, M., & Dawson, J. H. (1982) *J. Biol. Chem. 257,* 5496−5502.

Sono, M., Hager, L. P., & Dawson, J. H. (1991) *Biochim. Biophys. Acta 1078,* 351−359.

Sundaramoorthy, M., Terner, J., & Poulos, T. L. (1995) *Structure 3,* 1367−1377.

Thomman, H., Bernardo, M., Goldfarb, D., Kroneck, P. M. H., & Ullrich, V. (1995) *J. Am. Chem. Soc. 117,* 8243−8251.

Tian, W. D., Wells, A. V., Champion, P. M., Di Primo, C., Gerber, N., & Sligar, S. G. (1995) *J. Biol. Chem. 270,* 8673−8679.

Trittelvitz, E., Gersonde, K., & Winterhalter, K. H. (1975) *Eur. J. Biochem. 51,* 33−42.

Tsai, R., Yu, C. A., Gunsalus, I. C., Peisach, J., Blumberg, J., Orme-Johnson, W. H., & Beinart, H. (1970) *Proc. Natl. Acad. Sci. U.S.A. 66,* 1157−1162.

Unger, B. P., Gunsalus, I. C., & Sligar, S. G. (1986) *J. Biol. Chem. 261,* 1158−1163.

Wayland, B. B., & Olson, L. W. (1974) *J. Am. Chem. Soc. 96,* 6037−6041.

Weber, G. (1973) in *Molecular Biophysics,* (Pullman, B., & Weisbluth, M., Eds.) pp 369−396, J. Wiley & Sons, New York.

Wells, A. V., Li, P., Champion, P. M., Martinis, S. A., & Sligar, S. G. (1992) *Biochemistry 31,* 4384−4393.

White, K. A., & Marletta, M. A. (1992) *Biochemistry 31,* 6627−6631.

Yu, C. A., & Gunsalus, I. C. (1974) *J. Biol. Chem. 249,* 102−106.

BI961511U